Deep-Sea Research, Vol. 33, No. 3, pp. 305 to 322, 1986.
Printed in Great Britain.

0198-0149/86 $3.00 + 0.00

The effect of rotation on intrusions produced by heating a salinity gradient

T. K. CHERESKIN*† and P. F. LINDEN*

(*Received* 5 *November* 1984; *in revised form* 20 *August* 1985; *accepted* 9 *September* 1985)

Abstract—Laboratory experiments which examine the effect of rotation on the intrusions produced by the sidewall heating of a salinity gradient are discussed. The three-dimensional aspects of the growth of double-diffusive intrusions are described. Rotation introduces an azimuthal or along-front component of flow in addition to the radial or cross-frontal flow due to the horizontal growth of intrusions. The heights of intrusions were measured from shadowgraph photographs.

Nonrotating experiments were also made; it was found that for these experiments the intrusion thickness was equal to a constant times the scale height $\eta = \Delta\rho/(d\rho/dz)$ as in HUPPERT and TURNER (1980, *Journal of Fluid Mechanics*, **100**, 367–384). For the experiments with rotation, the parameter f/N was varied for fixed supercritical Rayleigh number (f is the Coriolis parameter; N is the buoyancy frequency). In the experiments with rotation, the intrusion thickness h increased up to the limit η for increasing f/N. The scales of the intrusions are interpreted in terms of the effect rotation has on the critical value of the Rayleigh number for the onset of intrusive layering. Results of a linear stability analysis which describe the onset of layer growth, and qualitative experiments for the Rayleigh number approaching critical are also discussed. A second type of instability was observed to occur concurrently with the double-diffusive layering. The initially symmetric growth of layers was observed to become unstable to nonaxisymmetric (azimuthal) disturbances. The observed wavelengths are comparable to wavelengths observed by GRIFFITHS and LINDEN (1982, *Geophysical and Astrophysical Fluid Dynamics*, **19**, 159–187) at the edge of a density-driven boundary current in a two-layer rotating fluid.

1. INTRODUCTION

OBSERVATIONS in the ocean over the past two decades have confirmed the presence of large-scale frontal interleaving where double diffusion appears to play an active role in the mixing of heat and salt between water masses (STOMMEL and FEDEROV, 1967; FOSTER and CARMACK, 1976; PERKIN and LEWIS, 1985). The main driving force of this interleaving is thought to be the lateral gradients of temperature and salinity across the front and vertical mass fluxes at intrusion interfaces (RUDDICK and TURNER, 1979; TOOLE and GEORGI, 1981). The gradients that occur in temperature and salinity are nearly compensating, suggesting that the very different diffusion rates of heat and salt play an important role in mixing. Both direct and indirect measurements have confirmed the presence of salt fingers on intrusion interfaces (WILLIAMS, 1975; MAGNELL, 1976; TOOLE, 1981), and horizontal mapping of the intrusions show cross-isopycnal slopes consistent with a double-diffusive driving mechanism (SCHMITT and GEORGI, 1982).

Although one-dimensional aspects of double-diffusive vertical transports have been

* University of Cambridge, Department of Applied Mathematics and Theoretical Physics, Cambridge CB3 9EW, U.K.
† Present address: College of Oceanography, Oregon State University, Corvallis, OR 97331, U.S.A.

studied extensively in laboratory experiments (TURNER, 1973), much remains to be learned about the two- and three-dimensional dynamics of the growth, maintenance and decay of intrusions. In the ocean the horizontal extents of these intrusions have been observed to be of order 10 to 20 km, with vertical scales from 2 to 70 m and lifetimes on the order of days or longer (STOMMEL and FEDEROV, 1967; SCHMITT and GEORGI, 1982). Recent measurements in the Arctic indicate horizontal extents on the order of hundreds of kilometres (PERKIN and LEWIS, 1985). Thus, to understand intrusive processes in the ocean, it is essential to look at the three-dimensional aspects of interleaving. In particular, for some of the large length and time scales that have been observed, the effect of the earth's rotation may have a significant effect on the growth of intrusions.

This paper presents the results of laboratory experiments which examine the effect of rotation on the intrusions created by the lateral heating of a salinity gradient. Several previous investigators have examined aspects of double-diffusive intrusions in the absence of rotation. TURNER (1978) produced intrusions by releasing, at its neutral buoyancy level, a source of fluid of one density into a volume of fluid with a density gradient (for example, sugar solution into a salt gradient). Initially, vigorous mixing occurred near the source, followed by the lateral spread of the mixed fluid at several depths. The main drawback of the experiment was the uncontrolled mixing at the source and hence unknown composition of the intruding fluid. RUDDICK and TURNER (1979) later made a set of carefully controlled experiments where they initiated interleaving by removing a barrier between a volume of sugar solution and one of salt solution, with matched surface and bottom densities and density gradients. If the density distributions on either side of the barrier are very nearly identical, the initial front, although distorted, is essentially vertical. However, this method of producing intrusions is extremely sensitive to even slight density mismatches, and rotation further complicates the problem of minimizing the initial disturbance due to removal of the barrier. The simplest and cleanest results have come from studies of intrusions that are produced from the sidewall heating (or cooling) of a salinity gradient. THORPE *et al.* (1969) and CHEN *et al.* (1971) used this technique to examine the effects of lateral gradients of temperature and salinity on the stability of thermohaline convection. HUPPERT and TURNER (1980) looked at both the heating and cooling of a salinity gradient to determine the vertical scales of double-diffusive intrusions, with application to the melting of icebergs. This method of creating intrusions has the advantage of a well-known initial condition and is relatively simple to set up in a symmetric geometry with rotation.

The intrusive layering in the experiment results from a double-diffusive convective instability. The source of the instability is from vorticity created in the following manner. Imagine a fluid with compensating horizontal gradients of temperature and salinity such that there is no net gradient in density. If we exchange two parcels of fluid at the same level, their temperatures will change much faster than their salt contents due to the faster diffusion of heat. Thus, the warmer, saltier parcel will cool and sink whereas the colder, fresher parcel will warm and rise, generating vorticity. In the case of sidewall heating of a salinity gradient, the rise of the fluid parcel is limited both by the slower diffusion of salt and the background gradient. A fluid parcel retains most of its salt as it rises, and so the vertical gradient limits the height to which a parcel can rise. A heated parcel can rise no more than

$$\eta = \Delta\rho \Big/ \left| \frac{d\rho}{dz} \right| = g'/N^2, \text{ where } \Delta\rho = |\rho(T_w, S_\infty) - \rho(T_\infty, S_\infty)|$$

and where

$$g' = g\Delta\rho/\rho_0 \text{ and } N^2 = -g/\rho_0\left(\frac{d\rho}{dz}\right)$$

and ∞ denotes the far-field; w denotes the wall value. The depth-averaged far-field salinity is S_∞; ρ_0 is the depth-averaged far-field density. When the heated fluid has risen to its neutral buoyancy level, it moves away from the wall into the interior where it cools and sinks. To conserve mass a pattern of convection cells is established with flow away from the wall at the top of the cells and toward the wall at the bottom. The simultaneous occurrence of cells along the wall and the existence of a preferred vertical scale or wavelength point to an instability phenomenon (THORPE *et al.*, 1969). Once established, the convective cells grow as intrusions into the interior of the fluid. In the laboratory the intrusions continue to grow until they reach the far wall of the container; they can be maintained for hours after their advance is halted by the far wall.

Other important forces are viscous forces and, in our case, the Coriolis force. Buoyancy forces from heating must overcome viscous forces before the heated fluid can rise, introducing a Rayleigh number criterion for the onset of convection based on the natural vertical scale η. The Rayleigh number is defined as

$$R = \left[g\eta^4\left(\frac{d\rho}{dz}\right)\right]/[\rho_0\kappa\nu] = [g(\Delta\rho)^4]/\left[\rho_0\kappa\nu\left(\frac{d\rho}{dz}\right)^3\right],$$

where κ is the molecular diffusivity of heat and ν is the kinematic viscosity. CHEN *et al.* (1971) determined the critical value of the Rayleigh number to be

$$R_{crit} = 15000 \pm 2500$$

for the onset of convection in a wide tank. For supercritical Rayleigh numbers, HUPPERT and TURNER (1980) found that the intrusion height, h, scaled with η. Specifically, they found that for $R \geqq 5 \times 10^5$, $h/\eta = 0.62 \pm 0.05$. As R approaches R_{crit}, h/η approaches unity.

Our experiments extend the above results for the sidewall heating problem by including the effects of rotation on the growth of intrusions. The Rayleigh number for most experiments was significantly supercritical to ensure the presence of vigorous intrusions, but some experiments were done with a Rayleigh number close to critical to look at the effect of rotation on the onset of growth. Rotation was seen to modify the stability criterion. It introduces a new source of vorticity from geostrophic shears that must be included in the balance of viscous dissipation and buoyancy production of vorticity. It also introduces a second length scale, the internal Rossby deformation radius. Additionally, three-dimensional effects were found to be important. Rotation introduces a geostrophic or along-front component of flow in addition to the ageostrophic cross-front flow due to the lateral growth of intrusions. The initially symmetric growth of layers was observed to become unstable to non-axisymmetric (along-front) disturbances. The growth of these disturbances will be compared with the experiments of GRIFFITHS and LINDEN (1982) which examined the instability of a density-driven boundary current in a two-layer rotating fluid.

2. EXPERIMENTS

The experiments were performed on a 1 m diameter, direct-drive rotating turntable. A rectangular tank measuring 45 by 60 cm in cross-section and 40 cm deep was used. The

tank was fitted with a centre brass cylinder 15 cm in diameter and 40 cm deep and centred on the vertical rotation axis of the table.

The space between the cylinder and the tank wall was filled with a linearly stratified salt solution, at room temperature, using the standard double-bucket procedure of OSTER (1965). Great care was taken with the filling procedure to ensure that the fluid was in a state of rigid-body rotation at the start of an experiment. (In a stratified fluid there will always be a small relative flow, commonly known as Eddington–Sweet circulation, caused by diffusion). The tank was filled slowly (about 1 cm height in 9 min) while rotating at the desired angular velocity. A styrofoam lid which floated up as the tank filled was used in many experiments to help the spin-up process. The depth of the fluid was usually less than the penetration depth given by WALIN (1969) for the spin-up of a stratified fluid ($D = fL/N$, where L is the tank radius). The spin-up was checked immediately prior to the start of each experiment by looking at the distortion of a vertical dye streak.

The tank was left for an additional 2 h after filling to allow the stratification to diffuse into a uniform gradient. Density was computed from refractive index using the polynomial fits given by RUDDICK and SHIRTCLIFFE (1979). The initial density gradient was calculated from a least squares linear regression of density vs height based on 5 to 8 samples drawn from fixed tubes mounted on the side of the tank. The linear gradients were quite good; correlation coefficients for the linear fit were 0.99 to 0.96.

Hot water of a given temperature was introduced into the centre cylinder and its temperature held constant by a heater. This temperature was measured again at the end of an experiment. The ambient tank temperature was measured at the start. Thermometer accuracy was 0.1°C.

Estimates of thickness of intrusions were made from shadowgraph photographs. These measurements are interpreted as 'space-averaged' since the shadowgraph integrates horizontally through the tank. Measurements always excluded the top and bottom layers which tended to be anomalous due to the boundaries. Several photos from each experiment were used. Additionally, layer heights in all experiments were estimated from distortions of a vertical dye streak. Plan-view observations were made by releasing dyed fluid at its neutral buoyancy level next to the heated sidewall.

3. OBSERVATIONS

Finite amplitude intrusions

These results describe the experiments where the Rayleigh number was large. For comparison, eight nonrotating experiments (those prefaced by 'S' in Table 1) were made with the same sidewall heating geometry as the experiments with rotation. Figure 1 is a shadowgraph photograph from one of these nonrotating experiments. Intrusions are characterized by sharp upper interfaces and less distinct lower interfaces, with turbulent mixing occurring within the layers. The downward component of flow at the top of an intrusion and the upward component of flow at the bottom of an intrusion give an overall downward slant to the layers. The lower interface is salt-fingering favourable, but salt fingers were not observed. The vigour of the convection within the intrusions may inhibit finger formation. The presence of large buoyancy fluxes produced by salt fingers would cause the intrusions to rise; in their absence the intrusions sink. Based on the eight nonrotating experiments, $h/\eta = 0.53 \pm 0.03$, a slightly smaller constant than that

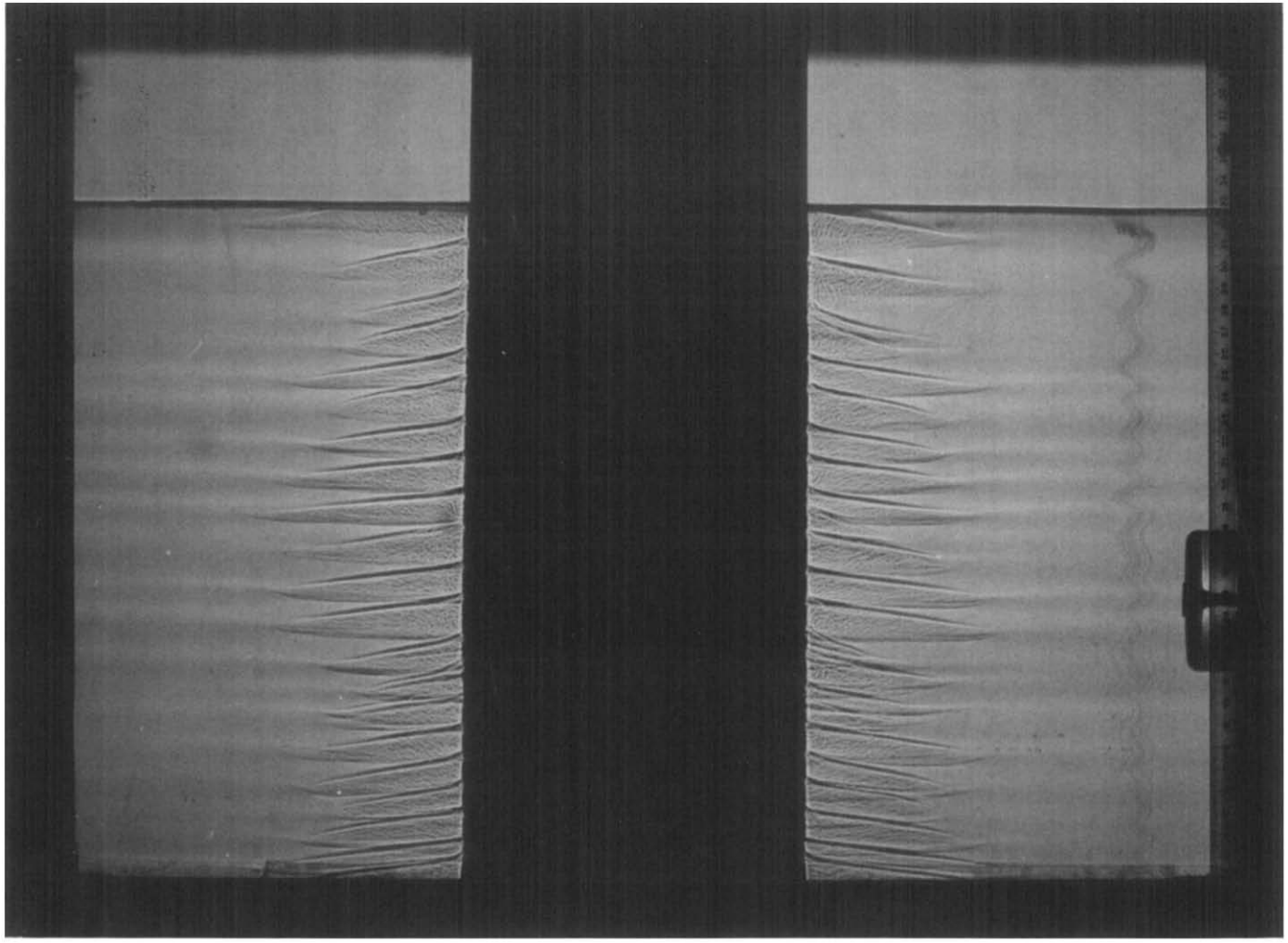

Fig. 1. Shadowgraph of sidewall heating in the absence of rotation. The dark column in the centre is the brass cylinder containing hot water. Temperature difference was 17°C; density gradient was 0.002 g cm^{-4}. The ruler on the side is marked in cm. Total depth is 32.5 cm. Photo was made 7 min after the start of the experiment.

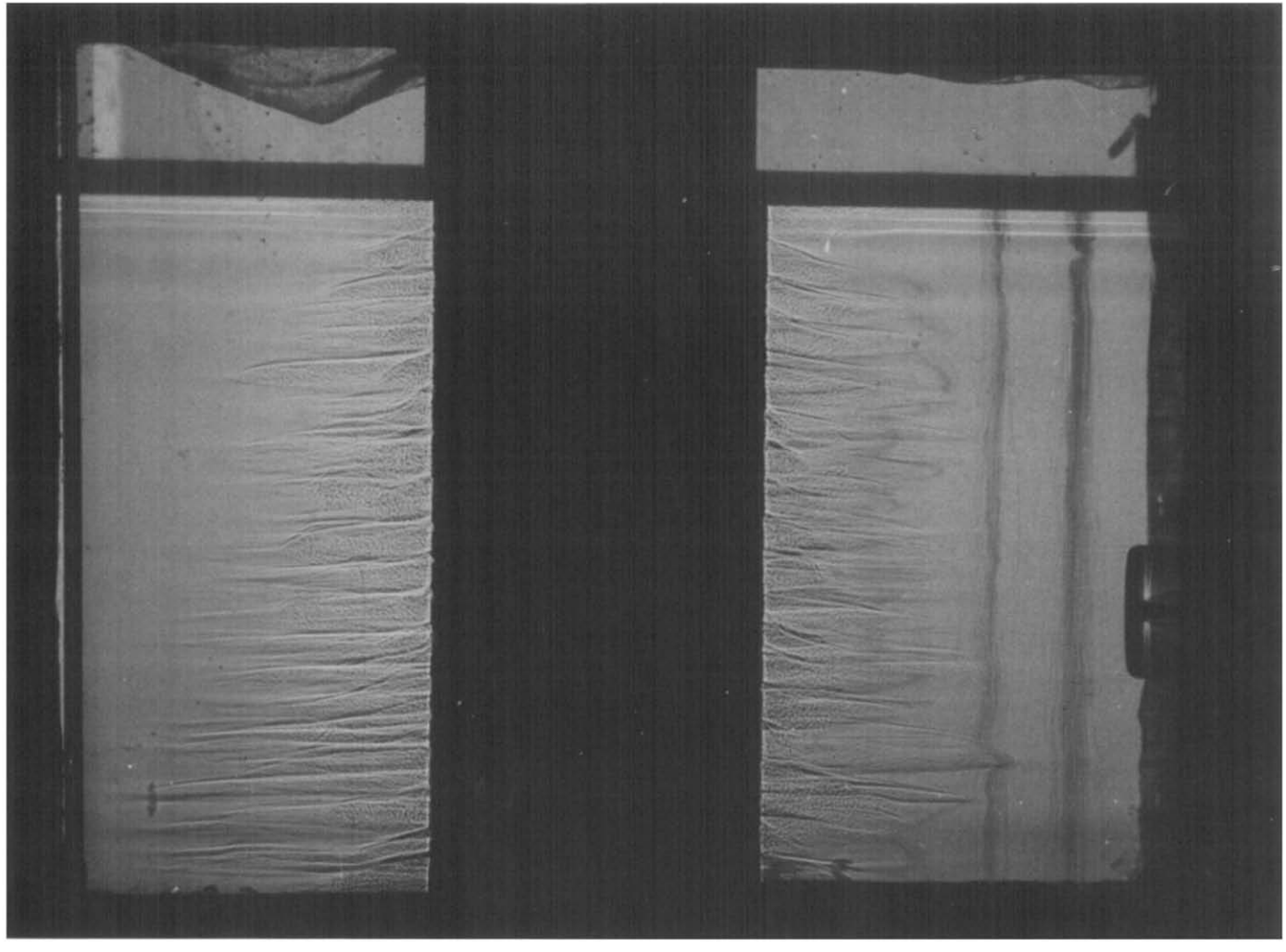

Fig. 2. Sidewall heating $f = 0.59$, experiment 11 at 5.5 min. Note how much less distinct the interfaces appear. On the right are two vertical dye columns which have not yet been reached by layers (experiment 11 in Table 1). Total depth is 34.6 cm.

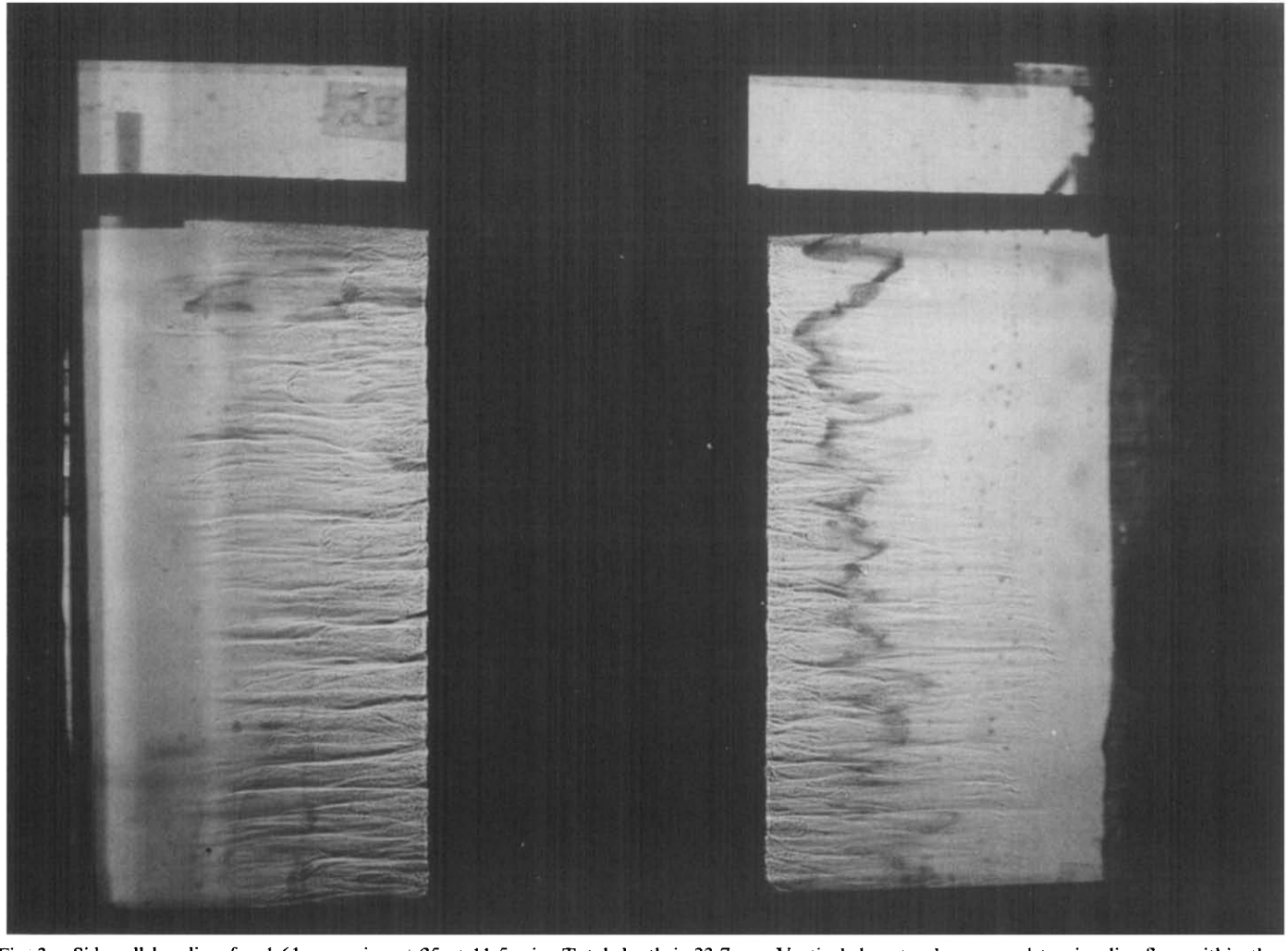

Fig. 3. Sidewall heading $f = 1.61$, experiment 25 at 11.5 min. Total depth is 33.7 cm. Vertical dye streak was used to visualise flow within the layers.

Table 1. *Experimental parameters and results from sidewall heating of a salinity gradient. The first group (prefaced by 'E') are experiments made with rotation. The second group (prefaced by 'S') are experiments made without rotation. Parameters are defined in the text.* f *is the Coriolis frequency,* N *is the buoyancy frequency,* $\Delta\rho$ *is the density change due to the sidewall heating,* r *is the mean background density,* h *is the measured intrusion thickness,* η *is the scale height,* L_η *is the Rossby radius based on* η, R *is the Rayleigh number (normalised by* 10^6*), and* T *is the Taylor number (normalised by* 10^4*). T is defined in equation (4.10); we used* d = η, n = 1, *and* $\nu = 0.01$ cm^2 s^{-1}

Exp.	f (s^{-1})	N (s^{-1})	$\frac{10^5\Delta\rho}{\rho}$	h (cm)	η (cm)	L_η (cm)	$\frac{R}{10^6}$	$\frac{T}{10^4}$
E21	0.32	1.31	496.5	1.6	2.82	11.67	7.70	0.07
E3	0.41	1.23	549.6	1.9	3.57	10.91	17.20	0.28
E2	0.50	1.20	561.6	1.8	3.81	9.05	21.40	0.54
E22	0.51	1.16	547.2	1.9	3.98	9.09	23.70	0.67
E24	0.51	1.11	343.3	1.9	2.75	5.87	4.90	0.15
E11	0.59	1.33	539.9	1.9	2.98	6.82	9.80	0.28
E14	0.80	1.18	515.5	1.7	3.60	5.29	16.60	1.10
E15	0.90	1.29	513.9	2.5	3.05	4.29	10.00	0.72
E20	1.11	1.37	587.0	2.4	3.05	3.83	11.50	1.09
E23	1.30	1.39	542.2	2.5	2.76	2.98	7.80	1.01
E25	1.61	1.41	456.1	2.9	2.24	1.93	3.50	0.67
E36	3.00	1.26	146.2	1.0	0.91	0.38	0.07	0.06
E37	4.50	1.31	134.7	1.1	0.77	0.22	0.04	0.07
S15	0.00	0.91	380.0	2.2	4.46	—	22.90	—
S16	0.00	1.15	400.0	1.5	2.96	—	7.10	—
S17	0.00	1.34	500.0	1.4	2.72	—	6.90	—
S19	0.00	0.93	340.0	2.2	3.90	—	13.90	—
S20	0.00	1.17	410.0	1.5	2.95	—	7.30	—
S21	0.00	1.39	500.0	1.4	2.57	—	5.80	—
S22	0.00	0.85	320.0	2.4	4.26	—	16.70	—
SJ7	0.00	1.31	500.0	1.45	2.84	—	7.80	—

observed by HUPPERT and TURNER (1980). The error bar is an estimate of the variation of individual thicknesses.

The growth of intrusions influenced by rotation can be summarised as follows. Heated fluid next to the cylinder rises until it reaches a level of neutral buoyancy, and then moves radially outward. At the top of the intrusion we see ageostrophic cross-frontal flow and a relative temperature maximum. To conserve angular momentum, an anticyclonic (along-front) flow is established in which the Coriolis force is balanced by the radial pressure gradient. Additionally, as the fluid moves outward it loses heat and sinks. At the bottom of the intrusions the flow is radially inward, and there are relative temperature minima. Conservation of angular momentum requires a cyclonic circulation at the bottom of a layer. Hence between the intrusive layering there is a pattern of alternating azimuthal flow with anticyclonic flow at the top of each layer and cyclonic flow at the bottom. The magnitude of the azimuthal flow decreases with increasing distance from the sidewall.

Qualitative observations of the lateral growth of intrusions indicate that rotation inhibits the radial component of flow. The initial growth of intrusions to the midpoint of the tank was similar to the rate of growth observed in the nonrotating experiments. However, the intrusions grew much more slowly as they advanced from the midpoint to the far wall. In some cases they did not reach the far wall by the end of an experiment (20 to 30 min), which never occurred in the experiments without rotation. The Coriolis force may be acting to convert radial flow into azimuthal flow. No azimuthal component of flow is observed in the experiments without rotation.

As in the nonrotating experiments, salt fingers are not observed to form on the lower interfaces, and intrusions appear to sink. However, the azimuthal flow introduces a three-dimensional aspect to the layering; dye observations indicate the layers spiral rather than merely slant downwards. Figures 2 and 3 are shadowgraph photographs from two different experiments with rotation. The upper interfaces of intrusions in experiments with rotation appear less distinct on the shadowgraph than do those in experiments without rotation. This effect may result from the three-dimensional aspect of the layering and the integral effect of the shadowgraph.

A plot of h/η vs f/N shows an increase in h with increasing f/N, limited by the scale height η (Fig. 5). A least squares linear regression of $\log(h/\eta)$ vs $\log(f/N)$ yields a slope of 0.4 with a correlation of 0.88.

$$h/\eta = (f/N)^{0.4}.$$

The effect of rotation in converting radial flow to azimuthal flow may result in keeping fluid against the sidewall and enabling layers to achieve a greater fraction of their maximum height. A second interpretation is that rotation increases the critical Rayleigh number, thus making the flow effectively less supercritical than the nonrotating Rayleigh number would indicate. HUPPERT and TURNER's (1980) results indicate that the layer

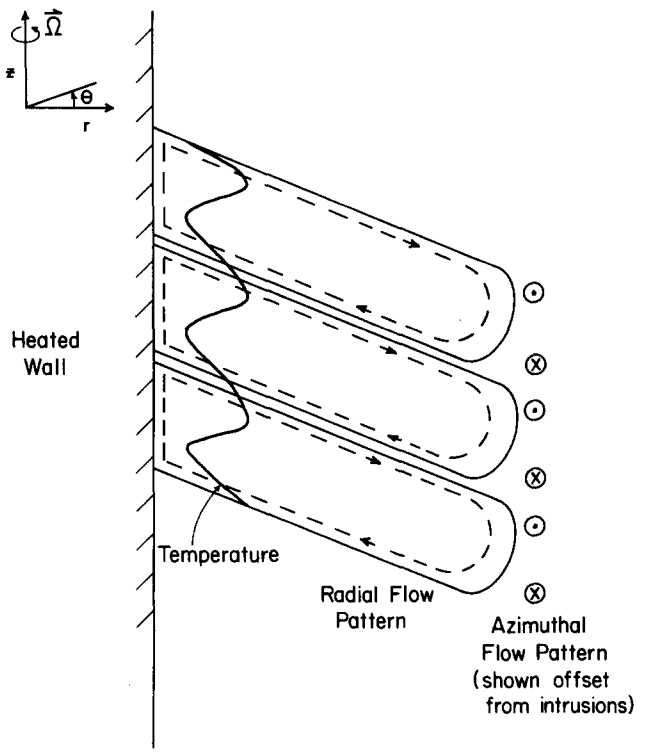

Fig. 4. Schematic of three intrusions growing outwards from a heated wall. The rotation is cyclonic. Prototype temperature trace shows temperature maxima occurring just below the top intrusion interface. Temperature minima occur just above the bottom interface. The arrows show the direction of the radial flow. For clarity the azimuthal flow is shown offset from the layers. Points are flowing towards the reader; crosses are flowing away.

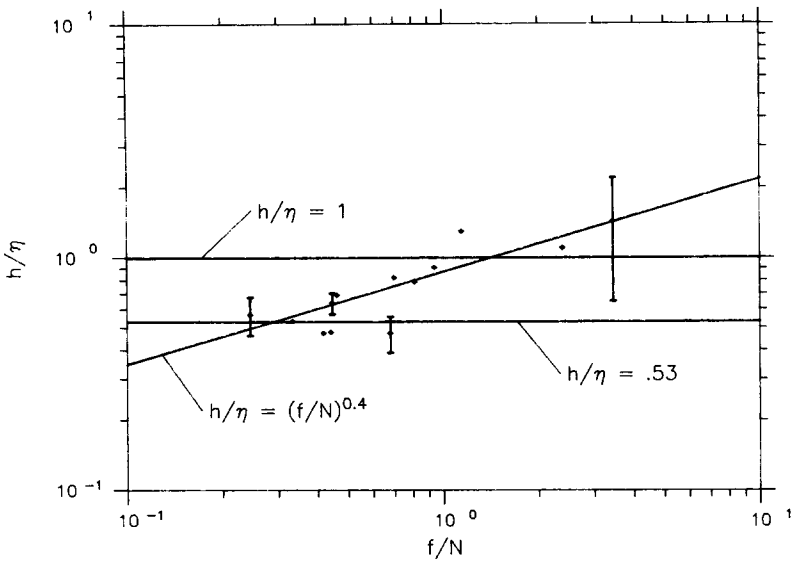

Fig. 5. Log-log plot of h/η vs f/N. Error bars are based on an estimate of the variation of individual layer thicknesses. Also shown are three lines: the nonrotating limit $h/\eta = 0.53$, the theoretical upper bound $h/\eta = 1$, and the least squares linear regression $h/\eta = (f/N)^{0.4}$.

height increases as the flow becomes critical. The effect of rotation on the critical Rayleigh number and the vertical wavenumber of the instability will be discussed more fully when we look at the onset of instability and the stability analysis sections.

High frequency variability is evident in the shadowgraphs of experiments with rotation; attempts to measure the layer thicknesses with a thermistor also gave evidence of this high frequency variability. The thermistor measurements could not distinguish between temporal and advective variations. A nonaxisymmetric disturbance was observed which did have a phase propagation relative to the rotating frame. However, although inconclusive, the observations seemed to indicate a higher frequency than due to advection of the nonaxisymmetric disturbance.

Nonaxisymmetric disturbances

Plan-view observations indicate that the initially symmetric growth of intrusions is unstable to nonaxisymmetric disturbances. The growth of these wave-like disturbances was observed when the horizontal spread was on the order of a Rossby radius. L_η, the Rossby radius based on η, is defined as

$$L_\eta = N\eta/f = g'/fN.$$

The wavelength of the disturbance is computed as $\lambda = 2\pi(R + L)/n$, where R is the inner cylinder radius, L is the horizontal width of the intrusion and n is the wavenumber. Observed wavenumbers ranged from 2 to 8; wavenumbers 3 and 4 were most frequently observed.

The nondimensional wavelengths of the disturbance are comparable to those observed by GRIFFITHS and LINDEN (1982). Their experiment looked at unstable buoyancy currents in a rotating two-layer fluid created by withdrawing the outer wall of an annulus with a

narrow gap. In our experiment we can think of the buoyancy current as being created from the sidewall heating. It is only in the crudest sense that this analogy holds since we have the added complications of a background gradient and double-diffusive instability.

The Froude number for our experiment is of order unity where the Froude number is defined as

$$F = (L/L_\eta)^2.$$

We find that wavelengths nondimensionalised by the deformation radius ranged from 2 to 5, which corresponds to the wavelengths observed at the edge of a buoyancy current with $F = 1$. GRIFFITHS and LINDEN's (1982) interpretation of their results pointed to a barotropic instability for $F < 1$ (current narrow compared to a Rossby radius) and primarily baroclinic for $F > 1$ (current wider than a Rossby radius). The disturbance we see for the sidewall heating problem may be a mixed barotropic/baroclinic instability since both horizontal and vertical shears are significant. The instability may be important in inhibiting the lateral spread of intrusions.

Onset of instability

A simple stability analysis indicates that rotation increases the value of the critical Rayleigh number for the onset of convection in a vertical slot. HUPPERT and TURNER (1980) found that h/η approached unity as the Rayleigh number approached critical. The trend for larger intrusion thicknesses with rotation may reflect an effect of the rotation making the flow less supercritical than in the absence of rotation. Estimates based on the following stability analysis indicate that rotation has a small effect for a narrow slot, but for a wide tank is could be as large as half an order of magnitude.

Some experiments included very fast rotation rates and low Rayleigh numbers to look at the effect of rotation on the onset of instability. Although the Rayleigh number was lowered to 2 to 4 times the critical value given by CHEN *et al.* (1971), double-diffusive convection still occurred, indicating that rotation does not change the critical value by an order of magnitude. Although intrusions did grow, the initial effect was dramatic, with the appearance of the initial roll cells retarded by 2 to 3 min. Normally these cells appear instantly when the sidewall heating commences. Additionally, the lateral growth rate was much smaller than for more vigorous intrusions at lower rates of rotation.

4. STABILITY ANALYSIS

To look at the effect of rotation on the onset of double-diffusive convection, we modified the stability analysis of THORPE *et al.* (1969). Their solution did not satisfy all the boundary conditions although it compared well with experiment. HART (1971) solved the problem with the correct boundary conditions and showed that to leading order the asymptotic solution for large Rz (defined below) yields the result found by THORPE *et al.* (1969). Both their experiments and ours were made with large values of Rz. We will follow the approach of THORPE *et al.* (1969) to make use of their graphical description for determining the critical Rayleigh number. To a first approximation rotation does not change the boundary layer solutions of Hart.

The problem that we consider is that of the gradual heating of a narrow slot. The slot will allow us to look at an initial state of no horizontal density gradient and hence no motion (ignoring Eddington–Sweet circulations). We are looking for the smallest

temperature difference sufficient to produce layering. Near a heated wall, the conduction of heat causes fluid to rise and isotherms to tilt. Since salt diffuses much more slowly, the rising fluid does not change salinity and establishes opposing tilts in the isohalines. If the heating is carried out sufficiently slowly and the slot is narrow, the horizontal density gradient will at all times be negligible. When the component horizontal gradients are sufficiently large, instability will occur in the form of double-diffusive layering. Although different from the wide tank problem of our experiment, we use this analysis to gain insight on the effect of rotation on the onset of the instability.

We start from a state of rest in a thin slot of width d (Fig. 6). The linearised equation of state is

$$\rho = \rho_0(1 - \alpha T + \beta S), \tag{4.1}$$

where ρ is the density, T is the temperature and S the salinity, α is the (positive) coefficient of thermal expansion and β is the (positive) coefficient representing the proportional density change per unit change in salinity at constant temperature. In the undisturbed state all gradients are assumed linear. Additionally, the undisturbed horizontal density gradient is zero such that

$$\alpha T_{0_x} = \beta S_{0_x} \tag{4.2}$$

where the subscript 0 indicates the unperturbed state and the vertical density gradient is negative (stable) such that

$$\beta S_{0_z} < 0. \tag{4.3}$$

The fluid is in solid body rotation with $f = 2\Omega$, where Ω is the uniform angular rotation rate. As mentioned above we also neglect the small motions produced by molecular diffusion in a rotating, stratified fluid (Eddington–Sweet flow).

Although the flow is three-dimensional, we will assume that there are no variations in the y-direction along the slot. The linearised, steady Boussinesq equations for the perturbations are:

$$\begin{aligned} -fv &= -p_x + \nu\nabla^2 u, \\ fu &= \nu\nabla^2 v, \\ 0 &= -p_z + (\beta S - \alpha T)g + \nu\nabla^2 w, \\ u_x + w_z &= 0, \\ uT_{0_x} &= \kappa\nabla^2 T, \\ uS_{0_x} + wS_{0_z} &= \kappa_S\nabla^2 S, \end{aligned} \tag{4.4}$$

where κ_s is the molecular diffusivity of salt and κ is the molecular diffusivity of heat. The boundary conditions are

$$\begin{aligned} u = v = w &= 0, \text{ on } x = 0, d, \\ S_x &= 0, \text{ on } x = 0, d, \\ T &= \pm\frac{1}{2}\Delta T, \text{ on } x = 0, d. \end{aligned} \tag{4.5}$$

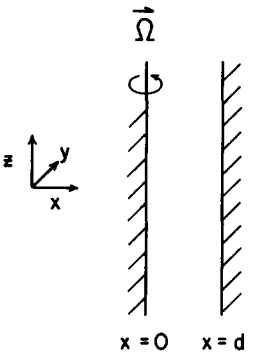

Fig. 6. Schematic of thin slot of width d.

We define a streamfunction based on the continuity equation,

$$(u, w) = (\psi_z, -\psi_x). \tag{4.6}$$

We formulate the equation for the horizontal vorticity and substitute the streamfunction to get a single equation in ψ.

$$\nabla^6\psi = -\frac{f^2}{\nu^2}\psi_{zz} + \frac{g}{\nu}\{(\beta S_{0_z}/\kappa_S)\psi_{xx} - (\beta S_{0_x}/\kappa_S - \alpha T_{0_x}/\kappa)\psi_{xz}\}. \tag{4.7}$$

This equation modifies that of THORPE *et al.* (1969) by the addition of a new term, $-f^2/\nu^2\ \psi_{zz}$; the new balance is between the production of vorticity by heating and by rotational shear on the one hand and the dissipation of vorticity on the other. The solution which satisfies $\psi = 0$ on the boundaries is given by THORPE *et al.* (1969) as

$$\begin{aligned}\psi &= \psi_0\{\cos[(l + k)x + mz] - \cos[(l - k)x + mz]\} \\ &= 2\psi_0 \sin(kx) \sin(lx + mz).\end{aligned} \tag{4.8}$$

Substitution yields the following two conditions

$$k = \frac{\pi n}{d},\ n \text{ integer};$$

$$[(l + k)^2 + m^2]^3 = -\frac{f_2}{\nu^2}m^2 + \frac{g\beta S_{0_z}}{\nu\kappa_s}(l \mp k)^2 - \frac{g}{\nu}\left(\frac{\beta S_{0_x}}{\kappa_s} - \frac{\alpha T_{0_x}}{\kappa}\right)(l \mp k)m. \tag{4.9}$$

If we scale by the slot width, $d/n\pi$, and define the following parameters

$$L = \frac{ld}{n\pi},\quad M = \frac{md}{n\pi},\quad T = \frac{f^2d^4}{\nu^2\pi^4n^4},$$

$$Rx = \frac{gd^4\beta S_{0_x}}{n^4\pi^4\nu\kappa_s} - \frac{gd^4\alpha T_{0_x}}{n^4\pi^4\nu\kappa}, \tag{4.10}$$

$$Rz = \frac{gd^4\beta S_{0_z}}{n^4\pi^4\nu\kappa_s},$$

the relation can be written as

$$[(L \mp 1)^2 + M^2]^3 = Rz(L \mp 1)^2 - Rx(L \mp 1)M - TM^2. \tag{4.11}$$

First we note that this is the same criterion obtained by THORPE *et al.* (1969) with the addition of a new term of positive definite sign, TM^2. A fixed value of this term implies that a larger rotation rate (T) implies larger layer heights (smaller M). THORPE *et al.* (1969) determined the minimum value of Rx which satisfied (4.11) and the corresponding values of L and M for a given value of Rx. We will do the same, for fixed values of T as well.

We rewrite the equations as follows

$$(p^2 + q^2)^3 = Rz\, p^2 - Rx\, pq - Tq^2,$$
$$p = L \mp 1,\ \mathrm{q} = M, \tag{4.12}$$

and parameterise by putting $p = aq$ so that

$$p^4 = \frac{Rz - aRx - a^2T}{(1 + a^2)^3},$$

$$q^4 = a^4 \frac{Rz - aRx - a^2T}{(1 + a^2)^3}, \tag{4.13}$$

(and $p = q = 0$). The curve defined by equations (4.13) corresponding to $T > 0$ lies totally inside the curve corresponding to $T = 0$ (Fig. 7). At $a \approx 0$, $p = q = 0$ for all T and these two curves are coincident. They slowly diverge as a approaches unity, where $p = q$. As a approaches infinity, p and q approach the origin. However, for nonzero T, p becomes imaginary before reaching the origin and the curve is discontinuous. The equations are symmetric with respect to the origin.

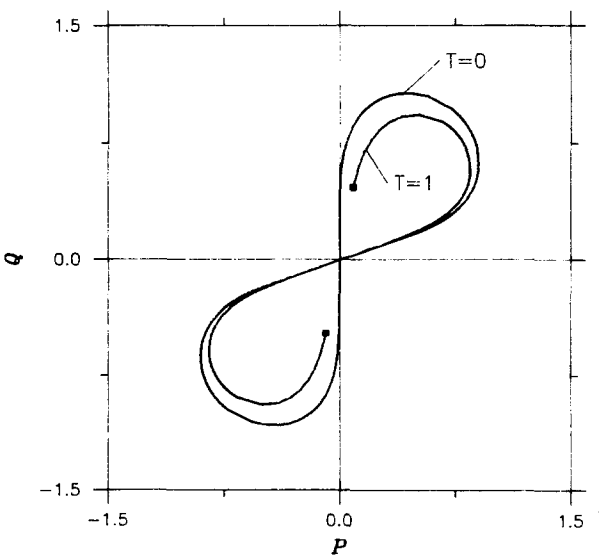

Fig. 7. Curve (4.13) for $Rx = -6$, $Rz = -2$. $T = 0$ is the outer curve; $T = 1$ is the inner curve.

In the (L, M) plane two curves are defined by (4.11) corresponding to the single curve in the (p, q) plane, and the minimum value for Rx for which there are simultaneous solutions of (4.11) is, in general, that value for which the two curves just touch. Because when $T > 0$ the curves lie inside the $T = 0$ curves, we can see qualitatively that the curves will need a larger value of Rx in order to touch (Fig. 8).

Quantitatively, a good approximation of when the curves first touch for $T = 0$ is when the left hand curve touches the line $L = 1$. From (4.12) we find that $dp/da = 0$ when

$$(5a^2 - 1)Rx + (4a^3 - 2a)T - 6aRz = 0, \tag{4.14}$$

and the condition that the curve (4.14) touches $p = 2$ is that (4.14) is satisfied and $p = 2$:

$$16(1 + a^2)^3 = Rz - aRx - a^2T. \tag{4.15}$$

This yields the following parametric form of the stability curve

$$\begin{aligned} Rx &= -2a\,\{48(1 + a^2)^2 + T\}, \\ Rz &= -16\,(5a^2 - 1)(1 + a^2)^2 - a^2T. \end{aligned} \tag{4.16}$$

For the case $T = 0$, this is the approximation for the neutral stability curve used by THORPE *et al.* (1969). For $T > 0$ (4.14) still yields the maximum of p with respect to a. The second condition ($p = 2$) underestimates the value of Rx when the curves first touch. Although the nonzero T curve is discontinuous through the origin, there does appear to be a simultaneous solution for the two curves. As we increase Rx for fixed T and Rz, we both increase the maximum of p with respect to a and extend the curve at large a further towards the origin.

We have plotted (4.16) in Fig. 9. Although the effect for small T is slight, there is again evidence that the effect of rotation is to increase the magnitude of Rx, the minimum critical Rayleigh number for the onset of convention. The magnitude of Rz, reflecting

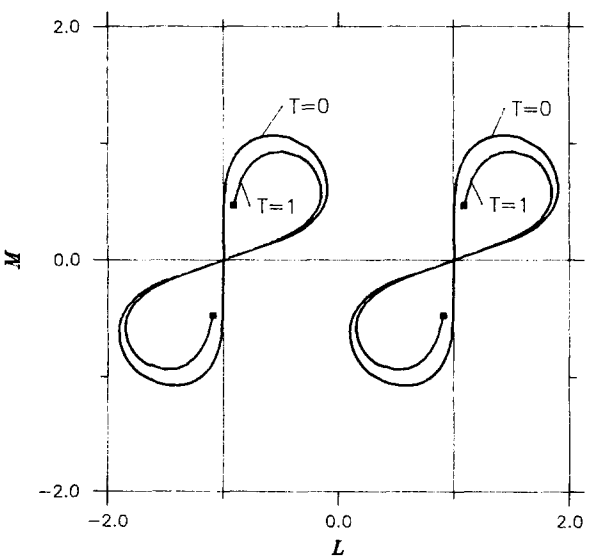

Fig. 8. Curve (4.13) in L, M plane for $Rx = -6$, $Rz = -2$.

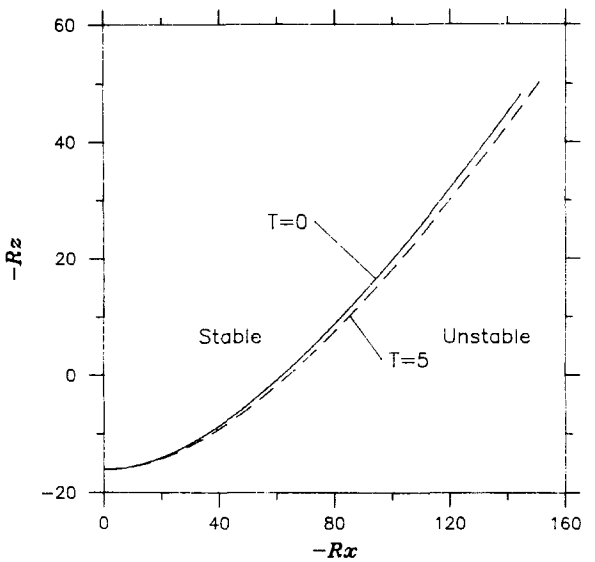

Fig. 9. Stability curve (4.16). Solid line is $T = 0$. Dashed line is $T = 5$.

background stability, is also increased by rotation. For a narrow slot ($d = 6$ mm) similar to that used in the experiments of THORPE *et al.* (1969) and a value of $f = 1$, the value of T is small, of order 10. However for convection in a wide tank where $d = \eta$, $T = 10^4$, and can increase Rx by a half order of magnitude.

5. CONCLUSIONS

Rotation was found to introduce several important modifications to the growth of double-diffusive intrusions. The flow was observed to be three-dimensional rather than two since rotation establishes an azimuthal flow resulting in a vertical azimuthal shear between the layers. The interfaces of the intrusions were unsteady. The intrusion thicknesses scaled differently and grew more slowly than those observed in the absence of rotation. The initially symmetric lateral growth of the layers was unstable to nonaxisymmetric disturbances. These disturbances began to grow when the lateral spread of the intrusions was on the order of a Rossby radius. The wavelength of the disturbances compared well with the wavelengths observed at the edge of a density-driven boundary current. It seems likely that the disturbance is a mixed barotropic/baroclinic instability deriving energy from the horizontal and vertical shears.

In addition to this new stability, rotation was found to change the critical Rayleigh number for the onset of the double-diffusive layering. The effect of rotation was stabilising. From a simple stability analysis rotation acts to increase the value of the Rayleigh number required for the onset of convention. We find h/η approaches 1 as f/N increases. In terms of the criticality of the flow, this is similar to the observation by HUPPERT and TURNER (1980) that h/η approaches 1 as R approaches R_{crit}. For a thin slot, the problem examined for the stability analysis, rotation probably does not change the Rayleigh number significantly. For layering in a wide tank, rotation could change the

critical value by as much as half an order of magnitude. This is consistent with experiments done at low Rayleigh numbers (but above critical) with very fast rotation rates where the onset of intrusion growth was retarded but still occurred.

Although for the most part oceanic values of f/N are smaller than those in the experiments, there are situations where similar conditions arise. The deep ocean and situations with enhanced background vorticity (e.g. due to eddies) are both examples of higher f/N values.

Acknowledgements—This work was supported by a grant from the Natural Environment Research Council. We thank D. Cheesley, D. Lipman, J. Sharpe and B. Wooten for their help with the experimental apparatus. We also thank G. Parker and J. E. Simpson for help with the photography. Comments and criticism from J. D. Milliman and the reviewers greatly improved the manuscript. T. Chereskin acknowledges the support of the Office of Naval Research contract N00014-84-C-0218 while this paper was written.

REFERENCES

CHEN C. F., D. G. BRIGGS and R. A. WIRTZ (1971) Stability of thermal convection in a salinity gradient due to lateral heating. *International Journal of Heat and Mass Transfer*, **14**, 57–65.

FOSTER T. D. and E. C. CARMACK (1976) Temperature and salinity structure in the Weddell Sea. *Journal of Physical Oceanography*, **6**, 36–44.

GRIFFITHS R. W. and P. F. LINDEN (1982) Laboratory experiments on fronts. Part I: Density-driven boundary currents. *Geophysical and Astrophysical Fluid Dynamics*, **19**, 159–187.

HART J. E. (1971) On sideways diffusive instability. *Journal of Fluid Mechanics*, **49**, 279–288.

HUPPERT H. E. and J. S. TURNER (1980) Ice blocks melting into a salinity gradient. *Journal of Fluid Mechanics*, **100**, 367–384.

MAGNELL B. (1976) Salt fingers observed in the Mediterranean outflow region using a towed sensor. *Journal of Physical Oceanography*, **6**, 511–523.

OSTER G. (1965) Density gradients. *Scientific American*, **213**, 70–76.

PERKIN R. G. and E. L. LEWIS (1985) Mixing in the West Spitzbergen Current. *Journal of Physical Oceanography* (to appear).

RUDDICK B. R. and J. S. TURNER (1979) The vertical length scales of double-diffusive intrusions. *Deep-Sea Research*, **22**, 509–515.

RUDDICK B. R. and T. G. L. SHIRTCLIFFE (1979) Data for double diffusers: physical properties of aqueous salt–sugar solutions. *Deep-Sea Research*, **26**, 775–787.

SCHMITT R. W. and D. T. GEORGI (1982) Finestructure and microstructure in the North Atlantic Current. *Journal of Marine Research*, **40**, *Suppl.*, 659–705.

STOMMEL H. and N. K. FEDEROV (1967) Small scale structure in temperature and salinity near Timor and Mindinao. *Tellus*, **19**, 306–325.

THORPE S. A., P. K. HUTT and R. SOULSBY (1969) The effects of horizontal gradients on thermohaline convection. *Journal of Fluid Mechanics*, **38**, 375–400.

TOOLE J. M. (1981) Intrusion characteristics in the Antarctic Polar Front. *Journal of Physical Oceanography*, **11**, 780–793.

TOOLE J. M. and D. T. GEORGI (1981) On the dynamics and effects of double-diffusively driven intrusions. *Progress in Oceanography*, **10**, 123–145.

TURNER J. S. (1973) *Buoyancy effects in fluids*. Cambridge University Press, 368 pp.

TURNER J. S. (1978) Double-diffusive intrusions into a density gradient. *Journal of Geophysical Research*, **83**, 2887–2901.

WALIN G. (1969) Some aspects of time-dependent motion of a stratified rotating fluid. *Journal of Fluid Mechanics*, **36**, 289–307.

WILLIAMS A. J. (1975) Images of ocean microstructure. *Deep-Sea Research*, **22**, 811–829.